

# Traveling Performance Evaluation for Planetary Rovers on Weak Soil

M. Sutoh, J. Yusa, K. Nagatani, K. Yoshida

Department of Aerospace Engineering, Tohoku University, Japan  
e-mail: {sutoh, yusa, nagatani, yoshida} @astro.mech.tohoku.ac.jp

## Abstract

Planetary rovers play a significant role in the surface explorations on the moon and/or Mars. However, because of wheel slippage, the wheels of planetary rovers may get stuck in loose soil. Therefore, in the design stage of planetary rovers, it is very important to consider wheel parameters such as wheel width and diameter to accomplish a given navigation mission. Typically, the wheel width and diameter are considered to be dominant factors of traversability of the wheel mechanism on loose soil. In order to quantitatively confirm the influence of these parameters on the traversability of planetary rovers, we performed experiments using a two-wheeled testbed on an inclined sandbox and carried out numerical simulations. In this paper, we report the experimental and simulation results, and discuss the influence of the wheel parameters on the traversability of wheels.

## 1 Introduction

During NASA's surface explorations on Mars, mobile robots (rovers) have played a significant role in geological investigations. In future missions, lunar and planetary rovers are also expected to have good performances for geological investigations. However, the surface of the moon and/or Mars is covered with loose soil, with many steep slopes along the rims of craters. Under such conditions, wheeled rovers may get stuck and, in a worst case scenario, such problems can cause the failure of the mission.

In order to avoid such problems, many research groups have studied the traveling performance of wheeled rovers on the basis of Terramechanics. This is a branch of mechanics that studies the interaction between soil and locomotion mechanisms on loose soil, which was systematized by M.G. Bekker and J.K. Wong in the 1970s [1]-[3]. On the basis of Terramechanics, our research group has also recently been studying the traveling performance of wheeled rovers [4]-[6].

In the design stage of planetary rovers, it is very important to consider wheel parameters such as wheel width and diameter that will enable the safe navigation of these rovers on loose soil. Evaluation tests of traversability using different wheel parameters are very helpful for such

wheel designs. However, only a few studies on the influence of wheel parameters on traveling performance have been reported. K. P. Pandey studied the influence of the wheel width and the lug length on the wheel's performance. However, the study used large target vehicles, such as dump trucks, and their behavior was different from that of planetary rovers [8]. K. Iizuka et al. reported the influence of the lug length on the traveling performance of small vehicles such as planetary rovers. However, they did not include the influence of the wheel diameter and width [9]. D. Gee-Clough studied the influence of the wheel diameter and the width on the rotational resistance of a small vehicle. However, the resistance was not enough to evaluate the traveling performance of planetary rovers [10].

In this study, we performed experiments to evaluate the influence of wheel parameters, in particular, the wheel diameter and the width, on the traveling performance of planetary rovers on loose soil. Generally, the traveling performance is evaluated on the basis of the relationship between the slip ratio and the slope angle (or drawbar pull). Therefore, we performed slope climbing tests for a two-wheeled testbed and measured the slip ratio of the wheels in a sandbox with different slope angles for 9 types of wheels. In this paper, we report the results of the above experiments, discuss the theoretical aspects, and introduce numerical simulation results to help understand the influence of wheel parameters on traveling performance.

This paper is organized as follows. Section 2 describes the method of evaluating the traveling performance. The two-wheeled testbed experiments are described in Section 3, along with an evaluation of the effects of the wheel diameter and the width on the traveling performance. The theoretical aspects and numerical simulations are discussed in Section 4, where the influence of wheel parameters on the traveling performance is addressed from a theoretical point of view.

## 2 Evaluation Method of Traveling Performance

One of the most important performance factors for planetary rovers is the ability to climb steep slopes that are covered with loose soil. To evaluate the ability of the wheel mechanism, we adopted the slip ratio as an indica-

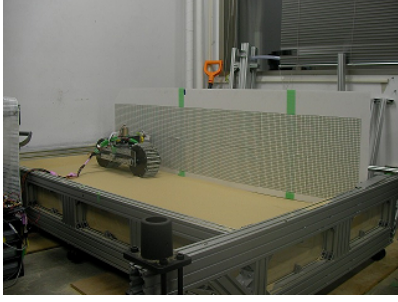


**Figure 1. Slope Climbing Test**

tor of climbing ability according to the slope angle. The slip ratio  $s$  is defined as [14]

$$s = \frac{v_d - v}{v_d} = 1 - \frac{v}{v_d} \quad (1)$$

where  $v$  denotes the longitudinal traveling velocity, and  $v_d$  denotes the circumference velocity of the wheel. In this equation, the slip ratio takes a value between 0 and 1. When the wheel moves forward without slippage, the slip ratio is 0; when the wheel does not move forward at all because of slippage, the slip ratio is 1. Therefore, a smaller slip ratio on a slope denotes a high traveling performance according to this definition.

### 3 Experiments

In this study, in order to evaluate the effects of the wheel width and diameter on the traveling performance on a slope, we performed slope climbing tests by using a two-wheeled testbed. In this experiment, 9 types of wheels were adopted, which have 3 types of wheel diameters and 3 types of wheel widths. In this section, details of the experiment are presented.

#### 3.1 Two-Wheeled Testbed

In this study, we developed a two-wheeled testbed where the wheel width and diameter can be changed by replacing its wheels. The wheel parameters and overviews of the two-wheeled testbed are listed in Table 1. The

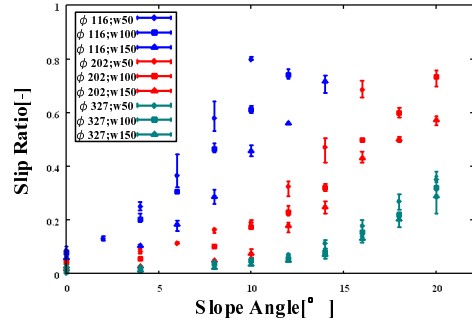


**Figure 2. Slope Angle vs. Slip Ratio (Entire Data)**

wheelbase of the testbed is fixed at 400 mm. To align the testbed weight to 6 kg for all the different wheels, we use additional weights. The wheels are equipped with parallel aluminum fins called lugs on their surface, to increase the drawbar pull. The lugs' length is determined such that it is proportional to the wheel diameter.

The testbed can rotate its wheels and control the velocity. The actual traveling velocity is obtained by visual odometry using a telecentric camera (TMMS: Telecentric Motion Measurement System) mounted on the testbed [7]. Thus, the slip ratio  $s$  is measured on-line by equation (1).

#### 3.2 Experimental Overview and Conditions

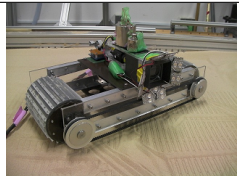
Each experiment was performed in our sandbox, which was covered with Toyoura sand. The sandbox had a length of 2 m, a width of 1 m, and a depth of 15 cm. This sandbox can be manually inclined to change its slope angle. The two-wheeled testbed with different wheels were used to perform traveling tests in the sandbox inclined at different slope angles (Fig. 1). We conducted three trials for each condition and measured the slip ratio after the sinkage of the wheels was stopped. The wheel velocity  $v$  was fixed at 2 cm/s in all the experiments. Slope angles were set at increments of 2° up to 20° for 9 types of two-wheeled testbeds.

#### 3.3 Experimental Results

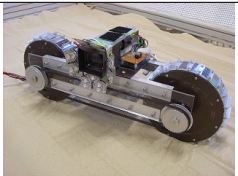
All the experimental results are plotted on the graph shown in Fig. 2. To evaluate the effect of the wheel diam-

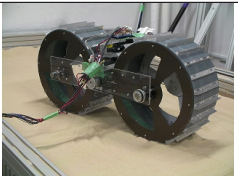
**Table 1. Wheel Parameters of Testbed**

	100-mm class	200-mm class	300-mm class
Diameter [mm]	116	202	327
Lug length [mm]	5	9	15
Width [mm]	50, 100, 150	50, 100, 150	50, 100, 150



Overview





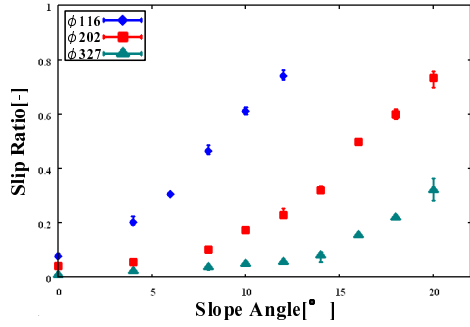


**Figure 3.** Slope Angle vs. Slip ratio  
(Wheel Width: 100 mm)

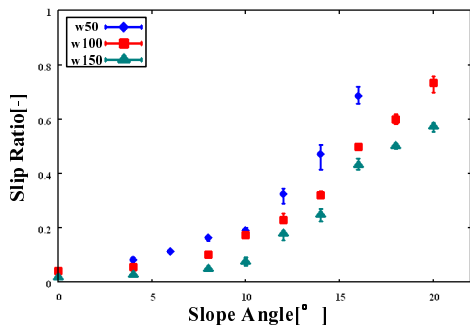
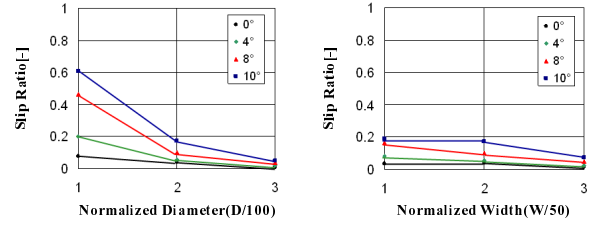


**Figure 4.** Slope Angle vs. Slip ratio  
(Wheel Diameter: 202 mm)

eter on the traveling performance, we extracted data for the case of a fixed wheel width of 100 mm from Fig. 2 and plotted them on the graph shown in Fig. 3. In order to evaluate the effect of the wheel width on the traveling performance, we extracted data for the case of a fixed wheel diameter of 202 mm from Fig. 2 and plotted them on the graph in Fig. 4. According to Fig. 3, the larger the wheel diameter is, the smaller the slip ratio on a slope becomes. This means that a large wheel diameter contributes to a high traveling performance. According to Fig. 4, the larger the wheel width is, the smaller the slip ratio on a slope will be. Therefore, a large wheel width also contributes to a high traveling performance.

Based on our analysis of the above results, the most important factor of traveling performance is the sinkage of the wheels. On loose soil, a wheel typically sinks into the soil when it rotates. The sinkage increases its traveling resistance and decreases its traveling performance. The sinkage depends strongly on the contact pressure. Therefore, a large diameter and width of a wheel will increase its contact area, causing a decrease in the contact pressure, and thus a decrease in its sinkage.

Next, we evaluate the impact of the relative size of the wheel width and diameter on the traveling performance. Fig. 5(a) shows the relationship between the wheel diameter and the slip ratio for a 100-mm-wide wheel. Fig. 5(b) shows the relationship between the wheel width and



(a) Diameter- Slip Ratio

(b) Width-Slip Ratio

**Figure 5.** Wheel Diameter/Width vs. Slip Ratio

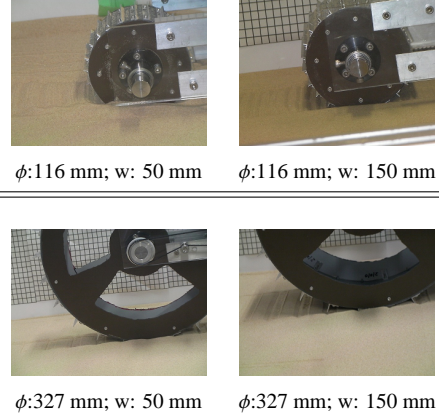


**Figure 6.** Wheel Sinkage (Slope Angle: 10°)

the slip ratio for a wheel diameter of 202 mm. In both the figures, the normalized wheel diameter or width denotes the ratio of the wheel diameter/width to the smallest wheel diameter/width. As shown in the figures, the slope of the wheel diameter vs. the slip ratio is steeper than that of the wheel width vs. the slip ratio, especially in case of large slope angles. Therefore, the wheel diameter seems to contribute to a high traveling performance, rather than the wheel width.

To discuss the above results, we consider the sinkage of the wheels. Fig. 6 shows photographs of wheel sinkage at a slope angle of 10° for different wheel diameters and widths. In the case of the wheel diameter of 116 mm, wheel sinkage changes comparatively according to the difference of wheel width. However, in the case of the wheel diameter of 327 mm, the wheel does not sink significantly with both wheel widths. Thus, the contact pressure between the wheel and the soil is sufficiently small in the case of the wheel diameter of 327 mm. Therefore, an increase in the wheel width has little effect on the traveling performance, especially in case of a large wheel diameter.

## 4 Numerical Simulation Based on Terramechanics

From the results of the experiments shown in the previous section, we concluded that the wheel diameter

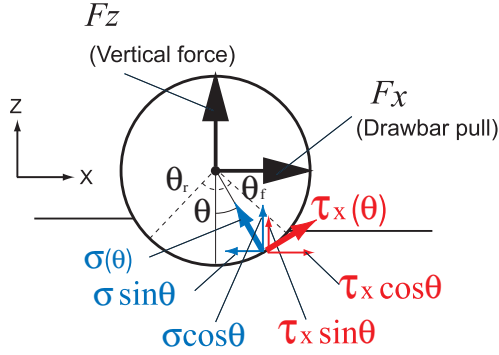


**Figure 7. Force Model of Wheel**

had more influence on the traveling performance than the wheel width. To discuss the validity of the results from a theoretical point of view, we describe a numerical simulation based on Terramechanics.

#### 4.1 Equations of Drawbar Pull and Vertical Force

In order to traverse a wheel on a slope covered with loose soil, a force that pulls the weight of the rover, called a drawbar pull, is required. At the same time, a weight-bearing force or a vertical force is required to prevent its sinkage into the soil. Generally, the traveling performance is determined by the relationship between the drawbar pull and the vertical force. Therefore, in this study, we performed a numerical simulation by calculating the drawbar pull  $F_x$  and the vertical force  $F_z$  using the Terramechanics models, and we compared the simulation results with the experimental results.

When a wheel rotates on loose soil, normal and shear stresses are generated under the wheel. These stresses are used in the calculation of the forces. According to Terramechanics models, the stresses are modeled, as shown in Fig. 7. Using the normal stress  $\sigma(\theta)$  and the shear stress  $\tau_x(\theta)$ , the drawbar pull  $F_x$  is calculated by integrating from the entry angle  $\theta_f$  to the departure angle  $\theta_r$  [2] as follows:

$$F_x = rb \int_{\theta_r}^{\theta_f} \{\tau_x(\theta) \cos \theta - \sigma(\theta) \sin \theta\} d\theta \quad (2)$$

and the vertical force  $F_z$  is obtained by the same method as described in equation (2) [2]:

$$F_z = rb \int_{\theta_r}^{\theta_f} \{\tau_x(\theta) \sin \theta + \sigma(\theta) \cos \theta\} d\theta \quad (3)$$

where  $b$  and  $r$  are the wheel width and wheel radius, respectively.

The normal stress  $\sigma(\theta)$  is determined by the following equation [1]:

$$\sigma(\theta) = \sigma_{max} \left( \frac{\cos \theta - \cos \theta_f}{\cos \theta_m - \cos \theta_f} \right)^n \quad (\text{for } \theta_m < \theta < \theta_r) \quad (4)$$

$$\sigma(\theta) = \sigma_{max} \left[ \frac{\cos\{\theta_f - \frac{\theta - \theta_r}{\theta_m - \theta_r}(\theta_f - \theta_m)\} - \cos \theta_f}{\cos \theta_m - \cos \theta_f} \right]^n \quad (\text{for } \theta_r < \theta < \theta_m) \quad (5)$$

where  $\theta_m$  is the specific wheel angle that the normal stress is maximized at

$$\theta_m = (a_0 + a_1 s) \theta_f, \quad (6)$$

where  $a_0$  and  $a_1$  are parameters that depend on the wheel-soil interaction. Their values are generally assumed as  $a_0 \approx 0.4$  and  $0 \leq a_1 \leq 0.3$  [2].

Based on the above, the maximum stress  $\sigma_{max}$  is modeled by the following terramechanics equation [2]:

$$\sigma_{max} = (ck_c + \rho k_\phi) \frac{r^n}{b^n} (\cos \theta_m - \cos \theta_f)^n \quad (7)$$

where  $k_c$ ,  $k_\phi$ , and  $n$  are the soil-specific parameters.  $\rho$  is the soil bulk density.

The shear stress  $\tau_x(\theta)$  is also expressed as [11]

$$\tau_x(\theta) = (c + \sigma(\theta) \tan \phi) [1 - e^{-j_x(\theta)/k_x}] \quad (8)$$

where  $c$  represents the cohesion stress of the soil,  $\phi$  is the internal friction angle of the soil, and  $k_x$  is the shear deformation module.  $j_x(\theta)$  is the soil deformation, which can be formulated as a function of the wheel angle  $\theta$  [11],

$$j_x(\theta) = r[\theta_f - \theta - (1 - s)(\sin \theta_f - \sin \theta)] \quad (9)$$

#### 4.2 Simulation Procedures and Conditions

The procedure to obtain the drawbar pull is summarized as follows.

1. Input the weight  $M$ , the wheel width  $b$ , the wheel radius  $r$ , and the slip ratio  $s$
2. Calculate the vertical stress  $\sigma(\theta)$  and the shear stress  $\tau_x(\theta)$  under the wheel from the stress distribution models described by equations (4) – (8)
3. Determine the entry angle  $\theta_f$  and the departure angle  $\theta_r$  when the vertical force  $F_z$  is equal to the normal load of the wheel, shown by equation (3)
4. Calculate the drawbar pull  $F_x$  using equation (2)
5. Go back to step 1

Simulations were carried out under the same conditions as were the experiments described in the previous section. The wheel weight was set to 3 kg to simulate the behavior of one wheel of the two-wheeled testbed. To match the simulation condition with that of the experiments, parameters of 9 types of wheels, 3 types of wheel widths, and 3 types of wheel diameters – are used. The soil parameters of Toyoura sand used in the simulations are listed in Table 2, as previously reported by our group[5].

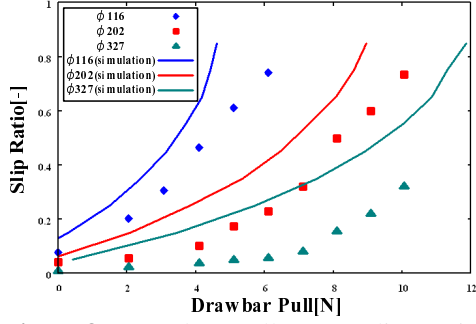


**Figure 8.** Drawbar Pull vs. Slip Ratio (Wheel Width: 100 mm)

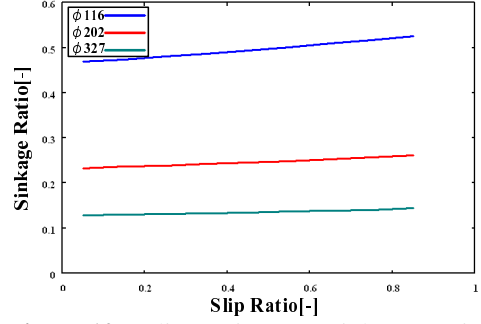


**Figure 10.** Slip Ratio vs. Sinkage Ratio (Wheel Width: 100 mm)

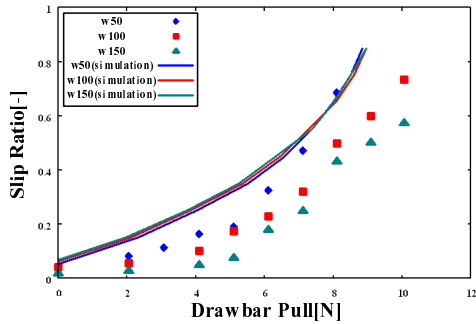


**Figure 9.** Drawbar Pull vs. Slip Ratio (Wheel Diameter: 202 mm)

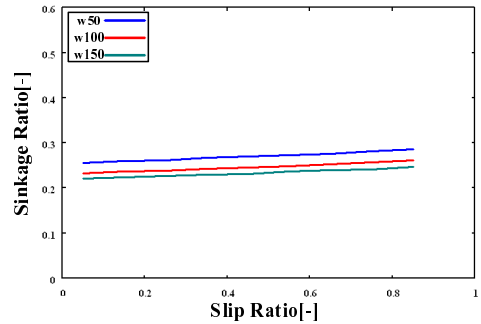


**Figure 11.** Slip Ratio vs. Sinkage Ratio (Wheel Diameter: 202 mm)

### 4.3 Simulation Results

To evaluate the effect of the wheel diameter on the traveling performance, we compare the simulation results with the experimental results. In Fig. 8, the smooth curves show the relationship between the simulated slip ratio and the drawbar pull for a 100-mm-wide wheel, with the experimental data superimposed on the graph. Here, the drawbar pull  $F_x$  in the slope climbing tests of the experiments was converted from the slope angle  $\theta$  using the following equation:

$$F_x = \frac{mg}{2} \sin \theta \quad (10)$$

**Table 2. Simulation Parameters and Values**

parameter	value	unit
$c$	0.0	[kPa]
$\phi$	38.0	[°]
$\rho$	1.49	[g/cm <sup>3</sup> ]
$k_x$	0.03	[m]
$k_c$	0.0	[N/m <sup>n+1</sup> ]
$k_\phi$	$1.20 \times 10^3$	[N/m <sup>n+1</sup> ]
$n$	1.70	[-]
$a_0$	0.4	[-]
$a_1$	0.15	[-]
$\kappa$	0.5	[-]

As shown in Fig. 8, the values of the simulations do not match with that of the experiments quantitatively. However, the general trends of the results, that the larger the wheel diameter, the smaller the slip ratio for a given drawbar pull is, match qualitatively. To evaluate the effect of the wheel width on the traveling performance in the simulation results, Fig. 9 depicts the relationship between slip ratio and drawbar pull as smooth curves for a 202 mm wheel diameter. To compare the simulation results with the experimental results, we superimpose the experimental data in Fig. 9. Here, the drawbar pulls of the slope climbing tests of the experiments were converted from the slope angles by equation (10). In Fig. 9, the trend of the simulation results is different from that of the experimental results. The simulation shows no effect of the increase in wheel width in the traveling performance.

### 4.4 Discussion

Our motivation for performing the above numerical simulation was to discuss the experimental results from a theoretical Terramechanics point of view. However, the simulation results, particularly regarding the effect of wheel width, showed a different trend from the experimental results, qualitatively. Therefore, in this section, we discuss the difference between the results of the numerical simulations and that of the experiment, particularly from the point of view of wheel sinkage.

Fig. 10, we depict the relationship between the slip ratio and the wheel sinkage ratio for a 100-mm-wide wheel, calculated by our numerical simulation. Furthermore, in Fig. 11, we depict the relationship between the slip ratio and the wheel sinkage ratio for a wheel diameter of 202 mm. The wheel sinkage ratio denotes the ratio of the wheel sinkage to the wheel radius. As shown in Fig. 10, the larger diameter of the wheel contributes to a smaller sinkage ratio. The above result matches the experimental observations, qualitatively. However, as shown in Fig. 11, the larger width of the wheel does not contribute much to the sinkage ratio according to the numerical simulations. The results of the numerical simulations indicate that the traveling performance does not improve by increasing the wheel width. However, this result does not agree with our observation in the experimental aspects, qualitatively.

Furthermore, in both figures, there is a slight increase in the sinkage ratio because of the increase in the slip ratio. In observations of the experiments, when a wheel slips on loose soil, the wheel scrapes the soil under it and sinks into the soil. It is observed that the larger the slip ratio is, the more dominant this effect appears. Thus, the trend of the relationship between the slip ratio and the wheel sinkage ratio in the simulations does not qualitatively match our observation in the experimental aspects.

In our simulation, wheel sinkage is simply obtained by a balance between the vertical force  $F_z$  and the normal force of the wheel. However, in the actual experiments, we observed that the lugs dig soil under the wheel when the wheel is slipping, which seems to increase the wheel sinkage. This effect is not included in our simulation model.

To summarize the above discussions, we confirmed that the large wheel diameter contributes to a high traveling performance based on our numerical simulation results. However, we did not confirm that the large wheel width also contributes to the performance. We believe that a new Terramechanics model is required to obtain more reasonable simulation results.

## 5 Conclusions

In this study, the evaluation method of traveling performance was defined, and two-wheeled testbed experiments were performed. From the results, we concluded that a large wheel diameter and a large wheel width contribute to a decrease in wheel sinkage into loose soil and to a high traveling performance. Moreover, we confirmed that a change in the wheel diameter contributes more to a high traveling performance than a change in wheel width. From the point of view of the simulation results, it was qualitatively validated that a larger wheel diameter contributes to a high traveling performance. However, our simulation model does not seem to be accurate enough to

represent wheel slippage, particularly the calculation of wheel sinkage.

In our future studies, we need to consider an optimal wheel diameter from the point of view of both the experiments and simulations. Moreover, we should discuss the lugs' effect on increasing the traveling performance. Reconstruction of the Terramechanics models is another important matter for future work.

## References

- [1] M. G. Bekker, "OFF-THE-ROAD LOCOMOTION", The University of Michigan Press, Ann Arbor, 1960.
- [2] J. Y. Wong, "Theory of Ground Vehicles", John Wiley & Sons, 1978.
- [3] J. Aizawa, N. Yoshioka, M. Miyata, Y. Wakabayashi, "Designing of Lunar Rovers for High Work Performance", *Proc. i-SAIRAS'99*, ESTEC, The Netherlands, June 1999, pp. 63–68.
- [4] K. Yoshida, H. Hamano, "Motion Dynamics and Control of a Planetary Rover With Slip-Based Traction Model", *SPIE 16th Int. Symp. on Aerospace/Defense Sensing, Simulation, and Controls*, SPIE4715-33, 2002.
- [5] K. Yoshida, N. Mizuno, G. Ishigami, A. Miwa, "Terramechanics-Based Analysis for Slope Climbing Capability of a Lunar/Planetary Rover", *24th Int. Symp. on Space Technology and Science*, June 2004.
- [6] G. Ishigami, A. Miwa, K. Nagatani, K. Yoshida: "Terramechanics - Based Model for Steering Maneuver of Planetary Exploration Rovers on Loose Soil", *The Journal of Field Robotics*, Volume 24, Issue 3, 2007, pp. 233-250.
- [7] K. Nagatani, A. Ikeda, K. Sato, K. Yoshida, "Accurate Estimation of Drawbar Pull of Wheeled Mobile Robots Traversing Sandy Terrain Using Build-in Force Sensor Array Wheel", *IEEE/RSJ Int. Conf. on Intelligent Robots and Systems*, pp. 2373-2378.
- [8] K. P. Pandey, T. P. Ojha, "Effect of Design Parameters on The Performance of Rigid Traction Wheels on Saturated Soils", *Journal of Terramechanics*, Vol 15, No 3, 1978, pp. 145–156.
- [9] K. Iizuka, Y. Kunii, T. Kubota, "Study on Wheeled Forms of Lunar Robots Considering Elastic Characteristic for Traversing Soft Terrain", *Journal of the Japan Society of Mechanical Engineers, Series C*, Vol 74, No 748, 2008, pp. 136–141.
- [10] D. Gee-Clough, "The Effect of Wheel Width on The Rolling Resistance of Rigid in Sand", *Journal of Terramechanics*, Vol 15, No 4, 1979, pp. 161–184.
- [11] Z. Janosi, B. Hanamoto, "The analytical determination of drawbar pull as a function of slip for tracked vehicle," *Proc of the 1st Int. Conf. on Terrain-Vehicle Systems*, Torino, 1961.